

Heat capacity of the high-temperature superconductor $\text{Ba}_2\text{DyCu}_3\text{O}_7$

Tooru Atake, Yoshiki Takagi, Tetsurō Nakamura, and Yasutoshi Saito

Research Laboratory of Engineering Materials, Tokyo Institute of Technology, 4259 Nagatsuta-cho, Midori-ku, Yokohama 227, Japan

(Received 24 August 1987)

The high-temperature superconductor $\text{Ba}_2\text{DyCu}_3\text{O}_7$ has been prepared, and characterized by electrical resistivity and dc magnetic susceptibility measurements. The heat capacity has been measured by an adiabatic calorimeter between 14 and 300 K. A typical second-order type of anomaly is observed due to the superconducting phase transition at 92.5 K. The heat-capacity jump at the transition point is obtained as $3.7 \times \text{JK}^{-1} \text{mol}^{-1}$ which leads to the electronic heat-capacity coefficient γ of $28 \text{ mJ K}^{-2} \text{mol}^{-1}$ in the weak-coupling limit of the Bardeen-Cooper-Schrieffer theory.

Since Ba-Y-Cu oxide was reported¹⁻³ to contain a superconducting phase with T_c above liquid-nitrogen temperature, many workers have studied this and related compounds, and several new high-temperature superconductors have been found so far: compounds represented as $\text{Ba}_2\text{XCu}_3\text{O}_7$ ($X=\text{Y, La, Nd, Sm, Eu, Gd, Dy, Ho, Er, Tm, Yb, Lu, etc.}$). Recently, increasing attention has been paid to the properties of the high-temperature oxide superconductors, especially to whether intrinsic bulk superconductivity or interfacial phenomena dominate in the ceramics. It is well known that the disappearance of electrical resistivity and even the observation of Meissner flux expulsion can result not from the bulk but from minor phases which exist as interfacial and/or grain-boundary portions throughout the sample. Thus, the question must be solved by measuring the heat capacity which shows a second-order type of anomaly due to the superconducting phase transition. The heat-capacity jump at the transition temperature is directly proportional to the amount of the superconducting phase. However, there have been few reports of calorimetric studies⁴⁻⁹ so far, and accurate thermodynamic properties up to room temperature have not been established yet. Such a situation has prompted the authors to start a series of thermodynamic studies on the high-temperature superconductors. Some results have been already published,^{8,9} in which clear heat-capacity jumps are observed in $\text{Ba}_2\text{YCu}_3\text{O}_7$ and $\text{La}_{1.85}\text{Sr}_{0.15}\text{CuO}_4$. This paper reports the results of heat-capacity measurements on $\text{Ba}_2\text{DyCu}_3\text{O}_7$ by adiabatic calorimetry between 14 and 300 K in an attempt to provide accurate equilibrium thermodynamic data.

The sample of $\text{Ba}_2\text{DyCu}_3\text{O}_7$ was prepared from a mixture of Dy_2O_3 , $\text{Ba}(\text{NO}_3)_2$, and CuO with the purities of 99.9%, 99.0%, and 99.99%, respectively. Appropriate amounts of the well-mixed constituent oxides were heated at 1173 K for 12 h in air. The sample was ground and mixed in an agate mortar and heated again. This process was repeated. The calcined powder was pressed into pellets, and then sintered at 1223 K for 16 h in oxygen atmosphere. After this procedure, the sample was cooled down to 1173 K for 1 h, 1073 K for 2 h, 973 K for 4 h, and then to room temperature at a cooling rate of 500 K h^{-1} in an oxygen atmosphere.

The final product was examined by x-ray diffraction, which showed the same structure as that of $\text{Ba}_2\text{YCu}_3\text{O}_7$ and confirmed its single phase. No trace of impurities was detected. A four-terminal dc resistivity measurement was also made on this sample. The temperature width of superconducting transition was 3.7 K.

The magnetic susceptibility and magnetization measurements were performed with a Faraday-type magnetic balance (model No. MB-2H, Shimadzu Co.) at 77 K. The sample was cooled to 77 K in a magnetic field of 0 T (zero-field cooling), and then the magnetization measurements were made by sweeping the magnetic field between zero to about 0.4 T. The magnetization data are shown in Fig. 1, where a remarkable feature is irreversibility of the magnetization curve. In Fig. 1 the initial measurements of increasing the magnetic field are denoted by the symbol \times , and those of decreasing the magnetic field by \circ . The subsequent series of measurements are indicated by different symbols: Δ, ∇ for increasing the magnetic field and \square, \bullet for decreasing the magnetic field. Both the shielding (increasing magnetic field) and the Meissner effects (decreasing) can be seen in the figure. The hysteresis phenomenon of magnetization suggests a flux-pinning effect due to some defects in the sample. The calibration of demagnetization coefficient for effective magnetic field and of paramagnetic term (extrapolated from magnetization values at higher temperatures than T_c) leads to the Meissner effect of 49% and lower critical field H_{c1} of about 0.1 T.

The heat capacities have been measured by using the laboratory-made adiabatic calorimeter which can work from 2 to 373 K. The adiabatic control is automated with five microvolt amplifiers (model No. AM1001B, Ohkura Electric Co.) and Proportional Integral Derivative (PID) control units (model No. 5301, Sinku-Riko, Inc.). The working thermometer mounted on the calorimeter vessel is a platinum resistance thermometer (type 5187L, H. Tinsley and Co., Ltd.) calibrated on the IPTS-68 between 13.81 and 373.15 K at the Nuclear Physics Laboratory in England. An ac automatic resistance bridge (type 5840D, H. Tinsley and Co., Ltd.) is used for the temperature measurements with the precision of $\pm 0.0001 \text{ K}$. For the energy measurements, a digital multimeter (model No.

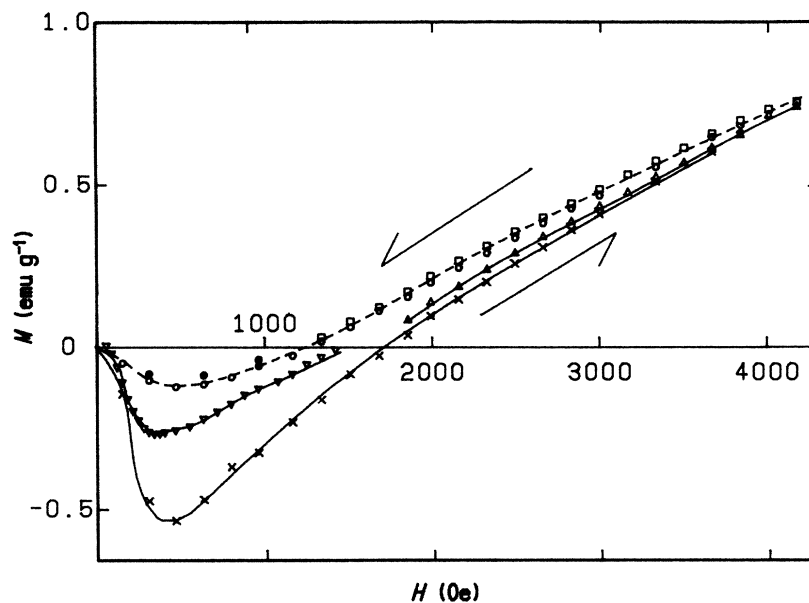


FIG. 1. Hysteresis loops of magnetization at 77 K for $\text{Ba}_2\text{DyCu}_3\text{O}_7$.

TR-6871, Advantest Co.), a universal scanner (model No. TR-7200), and a universal counter (model No. TR-5821) are used. All the instruments are equipped with GP-IB, and the system is automated by using a microcomputer (model No. PC-9801M2, NEC Corporation). Thus the heat-capacity values can be automatically obtained within the precision of $\pm 0.1\%$.

The amount of the sample loaded into the calorimeter vessel was 25.7335 g which corresponded to 0.034785 mol assuming the chemical formula as $\text{Ba}_2\text{DyCu}_3\text{O}_y$ ($y=7$). A small amount of helium gas (10 kPa at room temperature) was added to aid in thermal equilibration within the calorimeter vessel. The contribution of the sample to the total heat capacity including the calorimeter vessel was about 40%–50% at the temperature covered in this experiment. After each heat input was over, thermal equilibrium within the calorimeter vessel was attained in a few

minutes below 20 K; it increased as the temperature increased (about 10 min above 100 K). The heat input was performed in a few minutes to give rise to a temperature increment of about 1.5 K below 20 K. The time increased with increasing temperature, and thus it took about 0.5 h to obtain one measurement point of heat capacity above 100 K.

The heat capacity of $\text{Ba}_2\text{DyCu}_3\text{O}_7$ was measured between 14 and 300 K. The primary data of molar heat capacities without curvature corrections are shown in Fig. 2. A typical second-order type of anomaly is clearly seen at 92.5 K. The heat-capacity anomaly due to the superconducting phase transition is shown in Fig. 3 on an enlarged scale, where two series of measurements carried out with temperature increment of about 0.5 K are given.

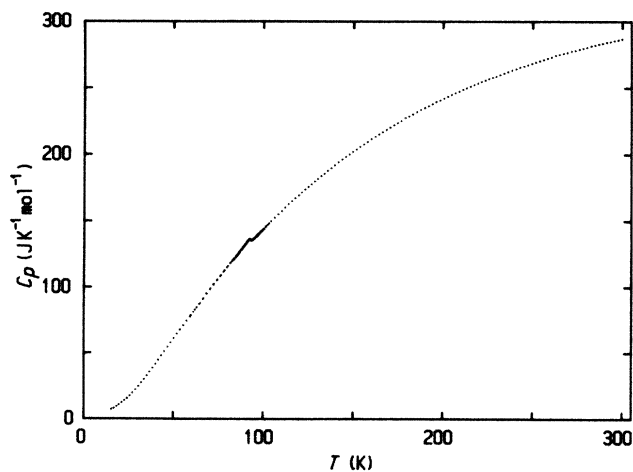


FIG. 2. Measured molar heat capacities of $\text{Ba}_2\text{DyCu}_3\text{O}_7$.

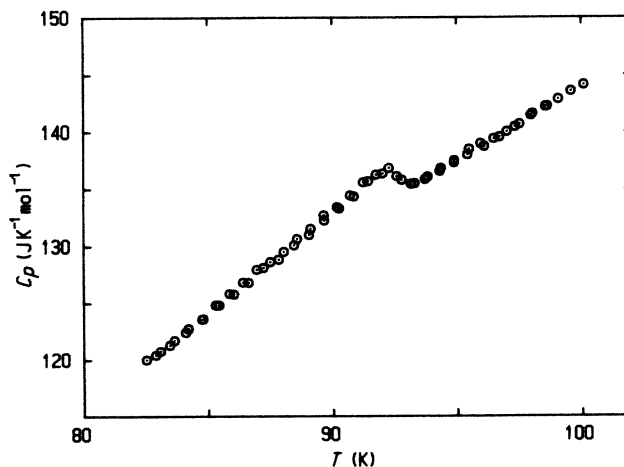


FIG. 3. Heat-capacity anomaly due to the superconducting phase transition at 92.5 K.

The heat-capacity jump at the transition temperature is obtained as $3.7 \text{ J K}^{-1} \text{ mol}^{-1}$, which leads to the electronic heat-capacity coefficient γ of $28 \text{ mJ K}^{-2} \text{ mol}^{-1}$ in the weak-coupling limit of the Bardeen-Cooper-Schrieffer theory. This value is twice as large as that of previous reports on $\text{Ba}_2\text{YCu}_3\text{O}_7$ ($\Delta C_p=2 \text{ J K}^{-1} \text{ mol}^{-1}$, $\gamma=15 \text{ mJ K}^{-2} \text{ mol}^{-1}$, $T_c=92 \text{ K}$) (Ref. 8) and $\text{La}_{1.85}\text{Sr}_{0.15}\text{CuO}_4$ ($\Delta C_p=0.6 \text{ J K}^{-1} \text{ mol}^{-1}$, $\gamma=11 \text{ mJ K}^{-2} \text{ mol}^{-1}$, $T_c=38 \text{ K}$).⁹

The most probable reason of such discrepancies lies in refinements in the sample preparation. The present results of $\text{Ba}_2\text{DyCu}_3\text{O}_7$ indicate the higher quality of the sample than the previous sample of $\text{Ba}_2\text{YCu}_3\text{O}_7$.⁸ In conclusion, therefore, it must be worth mentioning that the precise measurements of basic properties are desired on refined samples of high-temperature superconductors to

establish the theoretical scheme for the superconducting mechanism.

Another interesting feature obtained in the present results is that the lowest-temperature heat capacity of $\text{Ba}_2\text{DyCu}_3\text{O}_7$ is much larger than that of $\text{Ba}_2\text{ErCu}_3\text{O}_7$.¹⁰ While the two heat capacities agree very well above 100 K up to room temperature, below the transition temperature the heat capacity of $\text{Ba}_2\text{ErCu}_3\text{O}_7$ decrease less steeply than that of $\text{Ba}_2\text{DyCu}_3\text{O}_7$ as the temperature decreases. The difference is maximum $3.5 \text{ J K}^{-1} \text{ mol}^{-1}$ (6–7% of the total heat capacity) at 45 K. Below 45 K, however, the tendency reverses and the heat-capacity curves cross each other at about 25 K. The discrepancy increases as the temperature decreases; $\text{Ba}_2\text{DyCu}_3\text{O}_7$ has three times larger heat capacity than $\text{Ba}_2\text{ErCu}_3\text{O}_7$ at 14 K. More-detailed investigation into this phenomenon is under way.

¹M. K. Wu, J. R. Ashburn, C. J. Torng, P. H. Hor, R. L. Meng, L. Gao, Z. J. Huang, Y. Q. Wang, and C. W. Chu, *Phys. Rev. Lett.* **58**, 908 (1987).

²Z. Zhao, L. Chen, Q. Yang, Y. Huang, G. Chen, R. Tang, G. Liu, C. Cui, L. Chen, L. Wang, S. Guo, S. Li, and J. Bi, *Kexue Tongbao* (to be published).

³S. Hikami, T. Hirai, and S. Kagosima, *Jpn. J. Appl. Phys.* **26**, L314 (1987).

⁴B. D. Dunlap, M. V. Nevitt, M. Slaski, T. E. Klippert, Z. Sun-gaila, A. G. McKale, D. W. Capone II, R. B. Poeppel, and B. K. Flandermeyer, *Phys. Rev. B* **35**, 7210 (1987).

⁵L. E. Wenger, J. T. Chen, G. W. Hunter, and E. M. Logothetis, *Phys. Rev. B* **35**, 7213 (1987).

⁶K. Kitazawa, M. Sakai, S. Uchida, H. Takagi, K. Kishio, S. Kanbe, S. Tanaka, and K. Fueki, *Jpn. J. Appl. Phys.* **26**, L342 (1987).

⁷Y. Maeno, Y. Aoki, H. Kamimura, J. Sakurai, and T. Fujita, *Jpn. J. Appl. Phys.* **26**, L402 (1987).

⁸K. Kitazawa, T. Atake, H. Ishii, H. Sato, H. Takagi, S. Uchida, Y. Saito, K. Fueki, and S. Tanaka, *Jpn. J. Appl. Phys.* **26**, L748 (1987).

⁹K. Kitazawa, T. Atake, M. Sakai, S. Uchida, H. Takagi, K. Kishio, T. Hasegawa, K. Fueki, Y. Saito, and S. Tanaka, *Jpn. J. Appl. Phys.* **26**, L751 (1987).

¹⁰K. Kitazawa, T. Atake, H. Ishii, H. Sato, H. Takagi, S. Uchida, Y. Saito, K. Fueki, and S. Tanaka (unpublished).